HHS Public Access

Author manuscript

Mol Cancer Ther. Author manuscript; available in PMC 2019 October 01.

Published in final edited form as:

Mol Cancer Ther. 2018 October ; 17(10): 2091–2099. doi:10.1158/1535-7163.MCT-18-0038.

Co-Targeting the Cell Intrinsic and Microenvironment Pathways of Prostate Cancer by PI3Kα/β/δ inhibitor BAY1082439

Yongkang Zou[#1], **Zhi Qi**[#1], **Weilong Guo**[1], **Liuzhen Zhang**[1], **Marcus Ruscetti**[2,#], **Tanu Shenoy**[2], **Ningshu Liu**[3], and **Hong Wu**[1,2,*]

[1]The MOE Key Laboratory of Cell Proliferation and Differentiation, School of Life Sciences, Peking-Tsinghua Center for Life Sciences and Beijing Advanced Innovation Center for Genomics, Peking University, Beijing 100871, China

[2]Department of Molecular and Medical Pharmacology, University of California, Los Angeles, CA 90095, USA

[3]Bayer AG, Drug Discovery TRG Oncology, Muellerstrasse 178, 13353 Berlin, Germany

[#] These authors contributed equally to this work.

Abstract

Targeting the PI3K pathway is a promising strategy for treating prostate cancers with PTEN-loss. However, current anti-PI3K therapies fail to show long-lasting *in vivo* effects. We find that not only the PI3Kα- and PI3kβ-isoforms, but also PI3Kδ, are associated with the epithelial-mesenchymal transition (EMT), a critical process distinguishing indolent from aggressive prostate cancer. This suggests that co-targeting PI3Kα/β/δ could pre-empt the rebound activation of the parallel pathways induced by α- or β-isoform-selective inhibitor and prevent EMT. Indeed, BAY1082439, a new selective PI3Kα/β/δ inhibitor, is highly effective *in vivo* in inhibiting *Pten*-null prostate cancer growth and preventing EMT in the mutant *Pten/Kras* metastatic model. The anti-PI3Kδ property of BAY1082439 further blocks B cell infiltration and lymphotoxin release, which are tumor microenvironment factors that promote castration-resistant growth. Together, our data suggest a new approach for the treatment of prostate cancer by targeting both tumor cells and tumor microenvironment with PI3Kα/β/δ inhibitor.

Keywords

prostate cancer; PI3K inhibition; EMT; CRPC; tumor microenvironment

Introduction

Prostate cancer is among the most common malignancy in males, and the second leading cause of male cancer-related death in the Western world (1). Activation of the PI3K pathway,

[*]Corresponding author and contact information: Dr. Hong Wu, School of Life Sciences, Rm 106, Jin Guang Life Sciences Building, Peking University, No. 5 Yiheyuan Road, Beijing, China 100871, Phone: 86-10-6276-8720, hongwu@pku.edu.cn.
[#]Current address: Memorial Sloan Kettering Cancer Center, New York, NY

Disclosure of Potential Conflicts of Interest: The other authors declare no conflicts of interest.

either through loss-of-function mutations in the *PTEN* tumor suppressor gene or by gain-of-function alterations in components of the PI3K pathway, is associated with adverse outcomes of prostate cancer (2). Among the various PI3K isoforms, the PI3Kβ subunit is predominantly activated in PTEN-loss-induced prostate cancer in the genetically engineered *Pten* conditional knockout mouse model (*Pb-Cre*$^{+}$*;Pten*$^{L/L}$, CP model) (3, 4). However, selective inhibition of PI3Kβ showed no significant anti-tumor efficacy in *PTEN*-null prostate cancer cell lines due to compensatory activation of the PI3Kα isoform, while selective inhibition of the PI3Kα isoform resulted in rebound activation of PI3Kβ in breast tumors with a PIK3CA activating mutation (5–7). Therefore, simultaneously inhibiting both PI3Kα and PI3Kβ activities may be a promising strategy for the treatment of cancers with *PTEN* loss or PI3K activation.

The epithelial-to-mesenchymal transition (EMT) is a potential mechanism by which prostate cancer cells acquire lethal metastatic features and mediate therapeutic resistance (8–10). We have previously demonstrated that combined activation of the PI3K pathway by PTEN-loss and the MAPK pathway by KRAS^{mut} in the mouse prostate (*Pb-Cre*$^{+}$*;Pten*$^{L/L}$*;Kras*$^{R12D/L}$, CPK model) mimics late-stage metastatic prostate cancer with EMT features (11, 12). While prostate epithelial cells derived from the CPK model are highly sensitive to PI3K and MAPK inhibitors, CPK prostate cells with EMT and mesenchymal features are resistant to these treatments through an unknown mechanism (13).

Androgen deprivation therapy (ADT) is the mainstream treatment for prostate cancer. However, many patients progress to highly aggressive castration-resistant prostate cancer (CRPC) within 2 years (14). Various hypotheses for CRPC growth have been investigated, such as amplification, mutation and splice variants of the androgen receptor (AR) gene (14); crosstalk between the PI3K and AR signaling pathways (15, 16); EMT (8–11); and neuroendocrine differentiation due to lineage plasticity (17). Recently, the role of tumor infiltrating leukocytes (TIL) in prostate cancer and CRPC progression has been revealed (18, 19), suggesting that simultaneously targeting both cancer cell-intrinsic and tumor microenvironment pathways is crucial for the treatment of prostate cancer and preventing CRPC development.

In this study, we tested the *in vitro* and *in vivo* efficacy of BAY1082439 (20), a new, selective PI3K inhibitor with equal potency against PI3Kα/β/δ isoforms, in treating prostate cancer with PTEN-loss. We show that BAY1082439 targets the major nodes of *Pten*-null prostate cancer initiation, progression and castration-resistant growth.

Materials and Methods

Animals

Pb-Cre^{+}*;Pten*$^{L/L}$ and *Pb-Cre*$^{+}$*;Pten*$^{L/L}$*;K-ras*$^{G12D/W}$ mice were generated as described (4, 11). All animal experiment was approved by the Ethics Committee of the Peking University with ID LSC-WuH-1

Inhibitors

BAY1082439 was provided by Bayer AG. TGX-221, BYL-719, CAL-101, Azacitidine, Flutamide and rapamycin were purchased from Selleckchem.com.

Cell Culture

The LNCaP and PC3 cell lines were purchased from ATCC in 2014, no further cell line authentication was conducted by authors. The CaP2, CaP8, and CPKV cell lines were established and cultured as described (13, 21). Isolated splenic cells were cultured in RPMI-1640 medium with 10% FBS and stimulated with 10μg/mL LPS (sigma) and 1μg/mL anti-CD40 (biolegend).

Protein and RNA Analysis

Protein was extracted with 1% SDS-lysis buffer and separated by 10% SDS-PAGE. The following antibodies were used: Actin from Santa Cruz (sc-1616); P-AKT (4060), AKT (4691), P-S6 (5364), S6 (2317). P-ERK1/2 (4370), ERK (4695) from Cell Signaling Technology. RNA was extracted then reverse transcribed using Kit from Promega (LS1040) and Vazyme (R223–01). Quantitative PCR was achieved using Invitrogen SYBR Green Supermix.

In vitro drug treatment assays

The cell growth, apoptosis and cell cycle were determined using kits from Dojindo (CK08), BD Pharmingen (559783) and MultiSciences (CCS012). PKV cell drug treatment was performed as described (13). For Lta/Ltb assay, 2×10^4 cell was planted in 12-well plate with Lta/Ltb (from Peprotech, 5ng/ml), Flutamide (from selleck, 10μm), after 5 days, the cell was digested then the total cell number was counted by cell counting chamber.

In vivo drug treatment

BAY1082439 was dissolved in 0.1N HCL at 75mg/ml and orally administered at a dose of 50 or 75mg/Kg/day. The pharmacokinetic profile of BAY1082439 in mice exhibits very large volume of distribution (5.2–5.7 L/Kg), high clearance (15 L/h/Kg) and a T1/2 of 0.4 h.

For PC3 xenograft study, cells were cultivated according to ATCC protocol then harvested for transplantation in a subconfluent (70%) state. Approximately 3×10^6 cells suspended in 50% matrigel, were injected into the left flank of male nude mice. Tumors were allowed to grow to the size of 25 – 50 mm2 before randomized to vehicle or BAY1082439 treatment group.

Histology and IHC Analysis

HE and IHC staining was performed as described (4). The following antibodies was used: AR (sc-816) from Santa Cruz; Vimentin (5741), E-Cadherin (3195), P-AKT (S473) (4060), P-STAT3 (Tyr705) (9145), CD19 (90176) from Cell Signaling Technology; Anti-Ki67 (15580), Anti-αSMA (ab5694), B220 (553084) from Abcam.

Tissue Dissociation, Single-cell Suspension and FACS analysis/sorting

Single-cell suspensions from prostate tumor and spleen and FACS analysis were performed as described (19). The separation of epithelial, EMT and mesenchyme-like cancer cells from CPKV prostate tumor tissue was done as described (13).

Methylation profile analysis

Bisulfite sequencing libraries were prepared from separated epithelial, EMT and mesenchymal-like cancer cells of CPKV prostate tissues. The RRBS libraries were aligned by BS-Seeker2 (http://www.biomedcentral.com/1471–2164/14/774), and differentially methylated sites (DMS) were calculated by CGmapTools (https://doi.org/10.1093/bioinformatics/btx595).

The relationship between PI3Kδ expression and DNA methylation profile was obtained by analysis of 494 prostate adenocarcinoma sample data from cbioportal.org.com (TCGA, provisional datasets).

Accession numbers

Gene expression datasets of E/EMT/M prostate tumor cells are available at Gene Expression Omnibus (GEO) under accession numbers GSE67879. Methylation profile analysis data are available at sequence read archive (SRA) under accession numbers SAMN09389193.

Data Analysis

Graphpad Prism software was used to calculate means and standard deviations (SD). The Student's t-test or two-way ANOVA were used to determine statistical significant, and $p < 0.05$ was considered statistically significant.

Results

The PI3Kα/β/δ inhibitor BAY1082439 is more effective than PI3Kα- and/or PI3Kβ−selective inhibitors in blocking PTEN-null prostate cancer cells growing *in vitro*.

To test whether BAY1082439 (Fig. S1A) could achieve better efficacy by preventing rebound activation of the PI3K pathway, we treated PC3 and LNCaP cells, both PTEN-null human prostate cancer cell lines, with various concentrations of BAY1082439 for 72 hours. BAY1082439 effectively inhibited cell growth (Fig. 1A) by blocking the G1/S cell cycle transition and by inducing apoptosis (Fig. S1B-C). The PI3Kβ-specific inhibitor TGX-221 and the PI3Kα-specific inhibitor BYL-719 were significantly less effective in inhibiting cell growth and blocking the G1 to S transition (Fig. 1A; Fig. S1C). In isogenic PC3 *PTEN*-WT and *PTEN*-null cells, *PTEN*-null cells were three orders of magnitude more sensitive to BAY1082439 than WT cells (Fig. 1B), indicating a wide, *PTEN* status-dependent therapeutic window. In both human prostate cancer cell lines and the CaP8 and CaP2 cell lines derived from the CP mice (21), BAY1082439 prevented the feedback activation of the PI3K pathway and the rebound AKT phosphorylation seen with TGX-221 treatment (Fig. 1C and Fig. 1D), and demonstrated equal potency to inhibit cell growth as the combination of the PI3Kα and PI3Kβ inhibitors TGX-221 and BYL-719 (Fig. 1E).

BAY1082439 is effective in preventing *Pten*-null prostate cancer progression *in vivo*.

Based on the superior and sustainable activity of BAY1082439 to inhibit AKT phosphorylation of human and mouse PTEN-null prostate cancer lines (Fig. 1C-D), we tested the effect of BAY1082439 in vivo. CP mice were treated with 75 mg/kg of BAY1082439 daily, starting at 6 weeks when PINs form, and ending at 10 weeks when untreated tumors progress to localized adenocarcinoma (Fig. 2A). BAY1082439 was well tolerated over the course of the study (Fig. S2). In comparison to the vehicle controls, the BAY1082439 treatment group showed significantly decreased tumor size and P-AKT staining, nearly normal luminal architecture (Fig. 2B; Fig. S3A), and a significant reduction of Ki67-positive cells (Fig. 2C). Smooth muscle actin (SMA) staining indicated no local invasion in the BAY1082439 treatment group compared to vehicle controls (Fig. S3B). We also tested the effect of BAY1082439 on PC3 xenograft tumors in vivo, which harbors *PTEN* and *P53* mutations. BAY1082439 can significantly inhibit the human prostate cancer growth as compared to vehicle controls (Fig. 2D). Together, these results showed that BAY1082439 effectively prevented prostate cancer progression in the clinically relevant CP model and inhibit aggressive human prostate cancer cell growth *in vivo*.

The PI3Kδ isoform is up-regulated during the EMT process and can be effectively inhibited by BAY1082439.

We have previously demonstrated EMT and mesenchymal-like prostate cancer cells isolated from the CPK model (PKV cells) are more resistant to the PI3K/mTOR inhibitor PKI-587 and the MEK inhibitor PD0325901 than epithelial tumor cells isolated from the same *in vivo* model (13), suggesting that the response to targeted therapies is not solely dependent on their primary genetic alterations.

By analyzing RNA sequencing data derived from epithelial (E), EMT and mesenchymal (M)-like cancer cells of the CPK prostate tissue and PKV cell lines established from CPK prostate tumor (12, 13), we found that the expression of *Pik3cb* was down-regulated in M-like cancer cells, while the expression of *Pik3cd* (PI3Kδ) was increased in EMT cells and further enhanced in M-like cancer cells (Fig. 3A-B). The differential expression of *Pik3cd* is likely controlled by an epigenetic mechanism, as evidenced by reduced representation bisulfite sequencing (RRBS) analysis. The methylation level of *Pik3cd* promoter is decreased in M-like cancer cells, whereas Azacitidine treatment can increase *Pik3cd* expression in E cancer cells (Fig. 3C-D). We also explored the relationship between *Pik3cd* DNA methylation and mRNA expression levels in 494 prostate cancer clinical samples from the Cancer Genome Atlas (TCGA) dataset and found a negative correlation between DNA methylation of the *Pik3cd* and its mRNA level (Fig. 3E).

Corresponding to their higher expression of *Pik3cd*, both the EMT and M-like subpopulations were more sensitive to the PI3Kδ inhibitor CAL-101 than the epithelial subpopulation (Fig. 3F). Since BAY1082439 can potently inhibit PI3Kδ activity (Fig. S1), we tested whether BAY1082439 could target epithelial, EMT and M-like states. BAY1082439 effectively inhibited tumor cell growth in all three cell subpopulations with comparable activity to the combination of the PI3Kα, β and δ inhibitors BYL-719, TGX-221, and CAL-101 (Fig. 3G-H), suggesting that BAY1082439 inhibits epithelial

cancer cells preferentially with its PI3Kα/β activity and suppresses M-like cancer cells with additional activity against PI3Kδ.

The ability of BAY1082439 to inhibit epithelial as well as EMT and M-like cancer cells prompted us to test whether it could prevent EMT *in vivo*. Six-week-old CPK mice were treated with 75 mg/kg BAY1082439 daily for 4 weeks (Fig. 4A). Significant reduction in tumor weight was observed upon BAY1082439 treatment as compared to the vehicle group (Fig. 4B). While the vehicle-treated mice developed poorly differentiated invasive carcinoma, the BAY1082439-treated mice had PIN lesions as evidenced by intact SMA staining and a reduction in Ki67 index (Fig. 4C). Although EMT regions, defined by positive epithelial (E-cadherin) and mesenchymal (vimentin) markers, clearly appeared in vehicle-treated mice (Fig. 4D, circled areas in the right panels), no obvious EMT regions in BAY1082439-treated mice could be observed (Fig. 4D). These data reveal that BAY1082439 effectively prevents and/or delays EMT-mediated invasive carcinoma in CPK mice through inhibition of both epithelial and M-like cancer cells.

BAY1082439 can inhibit castration resistance tumor growth.

Given the strong inhibitory effects of BAY1082439 on the PI3K pathway and EMT, we tested its effect on CRPC growth. We castrated CP mice at 10 weeks of age when the animals develop invasive adenocarcinoma and compared castration resistant growth with or without BAY1082439 treatment 4 weeks later (Fig. 5A). As a control, we also performed similar treatment with rapamycin, an inhibitor targeting the PI3K downstream effector mTOR. After 4 weeks of castration, CP mice developed CRPC with increased Ki67-positive cells and diffuse AR staining (Fig. 5C). In contrast, the prostates from the mice treated with BAY1082439 showed significant inhibition of the PI3K pathway and tumor cell proliferation, as assessed by P-AKT level and Ki67 IHC, which led to significant reduction in tumor weight (Fig. 5B-C; Fig. S4). Although rapamycin could also reduce tumor weight (Fig. 5B), there were more Ki67 positive tumor cells compared to the BAY1082439-treated group (Fig. 5C).

BAY1082439 can block B cell infiltration and lymphotoxin-mediated survival signaling from tumor microenvironment.

Recent studies revealed that lymphotoxin produced by B cells, can promote CRPC growth (18). We also found increased B cell infiltration in castrated prostate tumor (Fig. S5A) and lymphotoxin can promote growth of cell line derived from CP mice tumor (Fig. S5B). Since PI3Kδ is important for B-cell receptor signaling (22), we hypothesized that BAY1082439 may be effective in suppressing PI3Kδ-driven B cell-dependent tumor-promoting signaling. Indeed, BAY1082439 was more effective at inhibiting the growth of freshly isolated splenic B cells *in vitro* when compared to the PI3Kδ-specific inhibitor CAL-101, while rapamycin had no obvious effect (Fig. S6A). Quantitative FACS and IHC analyses showed that compared to castrated mice, BAY1082439 treatment led to significantly decreased tumor infiltrating B cells (Fig. 6A; Fig. 6D; Fig. S6C) while the number of infiltrating CD8-positive T cells was not changed (Fig. S6B). *Cxcl13* expression, a B cell chemotactic chemokine, was decreased upon BAY1082439 treatment in the tumor lesion (Fig. 6B).

Furthermore, the mRNA levels of B cell-released lymphotoxin-α and β (*Lta* and *Ltb*) were significantly reduced in BAY1082439-treated tumor remnants (Fig. 6C).

Histologically, B220-positive B cells were surrounded by Ki67-positive tumor cells in the castrated and rapamycin-treated prostates (Fig. 6D, upper and lower panels). These Ki67-positive cells are almost absent in the BAY1082439-treated tumor remnants (Fig. 6D, middle panels), suggesting that infiltrating B cells may promote tumor growth. The LTA and LTB heterotrimer promotes androgen-independent growth via LTBR-mediated activation of IKKα and STAT3 phosphorylation (P-STAT3) (18). In line with reduced B cell infiltration and *Lta* and *Ltb* expression, we also observed that the P-STAT3 level was significantly reduced in castrated BAY1082439-treated prostates (Fig. 6E). However, the number of tumor infiltrating B cells, the *Cxcl13* and *Ltb* expression levels as well as the P-STAT3 level were not changed after rapamycin treatment (Fig. 6A-E), indicating that the CXCL13/lymphotoxin/P-STAT3 pathway may support CRPC growth in the rapamycin treatment group. Together, these results support the notion that BAY1082439 not only targets cancer cell-intrinsic proliferation and survival pathways by inhibiting PI3Kα and PI3Kβ, but also suppresses castration-induced EMT and inhibits B cell-driven tumor-promoting signaling pathways.

Discussion

Attempts at developing effective anti-PI3K inhibitors for the treatment of prostate cancer and other human cancers have been hindered by insufficient efficacy and/or therapeutic window (23–25) as well as the development of resistance mechanisms involving feedback and parallel pathways (5–7, 26). We demonstrate in this study that BAY1082439, a new PI3Kα/β/δ inhibitor, has much higher efficacy to inhibit PTEN-null prostate cancer cell growth than the α− and β-isoform specific inhibitors BYL-719 and TGX-221 by blocking the mutual feedback activation between PI3Kα and PI3Kβ. BAY1082439 also inhibits prostate cancer progression in preclinical *Pten*-null prostate cancer model and shows the therapeutic potential for aggressive human PC3 xenograft tumor i*n vivo*.

A recent study identifies an alternative spliced variant of the *PIK3CD* (*PIK3CD-S*) in prostate cancer specimen, which is associated with poor survival and resistant to CAL-101 (27). We show in this study PI3Kδ isoform is differentially expressed in epithelial, EMT and M-like cells by an epigenetic regulatory mechanism, and reveal that BAY1082439 effectively suppresses EMT-mediated cancer progression by blocking PI3Kδ. Further study is needed to study the potential alternative splice events in the *Pik3cd* and other cancer driver genes during EMT and M-like cells and test the sensitivity of BAY1082439 in human prostate cancers carry the *PIK3CD-S* variant.

Although most men initially respond to ADT, but its therapeutic benefits are short-lived, and some patients succumb to CRPC within 18–24 months (14). Here we show in *Pten*-null mouse model that co-inhibiting EMT and the PI3K pathway by BAY1082439 and shutting down AR signaling by castration leads to significant inhibition of CRPC growth. Recent studies have highlighted the potential role of tumor infiltrating B cells in CRPC development (18). Similar to subcutaneous Myc-CaP and spontaneous TRAMP mouse models (18), we

also observed significant increases in B cell tumor infiltration, lymphotoxin release and upregulated STAT3 signaling in our castrated *Pten*-null prostate cancer model. Importantly, BAY1082439, with its anti-PI3Kδ activity, can effectively reduce the number of infiltrating B cells and suppress lymphotoxin α/β release, STAT3 activation, and androgen-independent growth in castrated tumor tissue.

In summary, our results highlight the unique role of BAY1082439 in targeting multiple PI3K isoforms that are critical for prostate cancer progression and therapeutic resistance. BAY1082439 may also have considerable clinical benefit by avoiding the potential side effects caused when combining multiple isoform-specific inhibitors. Our results also suggest that co-targeting the cell-intrinsic and microenvironment pathways are essential for late stage prostate cancers and should be further explored.

Supplementary Material

Refer to Web version on PubMed Central for supplementary material.

Acknowledgments

We thank the Peking University Histology Core and Tsinghua University Flow Cytometry core for their assistance. This work was supported in part by the funds from Beijing Advanced Innovation Center for Genomics at Peking University as well as awards from the NIH (P50-CA092131 and U01-CA164188) and Bayer AG through the strategic alliance between Peking University and Bayer to HW.

This work is support in part by Bayer AG for HW. NL is an employee of Bayer AG.

Reference

1. Siegel RL, Miller KD, Jemal A. Cancer statistics, 2018. CA: a cancer journal for clinicians. 2018.
2. Taylor BS, Schultz N, Hieronymus H, Gopalan A, Xiao Y, Carver BS, et al. Integrative genomic profiling of human prostate cancer. Cancer cell. 2010;18:11–22. [PubMed: 20579941]
3. Jia S, Liu Z, Zhang S, Liu P, Zhang L, Lee SH, et al. Essential roles of PI(3)K-p110beta in cell growth, metabolism and tumorigenesis. Nature. 2008;454:776–9. [PubMed: 18594509]
4. Wang S, Gao J, Lei Q, Rozengurt N, Pritchard C, Jiao J, et al. Prostate-specific deletion of the murine Pten tumor suppressor gene leads to metastatic prostate cancer. Cancer cell. 2003;4:12.
5. Cescon DW, Gorrini C, Mak TW. Breaking up is hard to do: PI3K isoforms on the rebound. Cancer cell. 2015;27:5–7. [PubMed: 25584888]
6. Schwartz S, Wongvipat J, Trigwell CB, Hancox U, Carver BS, Rodrik-Outmezguine V, et al. Feedback suppression of PI3Kalpha signaling in PTEN-mutated tumors is relieved by selective inhibition of PI3Kbeta. Cancer cell. 2015;27:109–22. [PubMed: 25544636]
7. Costa C, Ebi H, Martini M, Beausoleil SA, Faber AC, Jakubik CT, et al. Measurement of PIP3 levels reveals an unexpected role for p110beta in early adaptive responses to p110alpha-specific inhibitors in luminal breast cancer. Cancer cell. 2015;27:97–108. [PubMed: 25544637]
8. Li P, Yang R, Gao WQ. Contributions of epithelial-mesenchymal transition and cancer stem cells to the development of castration resistance of prostate cancer. Molecular cancer. 2014;13:55. [PubMed: 24618337]
9. Sun Y, Wang BE, Leong KG, Yue P, Li L, Jhunjhunwala S, et al. Androgen deprivation causes epithelial-mesenchymal transition in the prostate: implications for androgen-deprivation therapy. Cancer research. 2012;72:527–36. [PubMed: 22108827]
10. Tanaka H, Kono E, Tran CP, Miyazaki H, Yamashiro J, Shimomura T, et al. Monoclonal antibody targeting of N-cadherin inhibits prostate cancer growth, metastasis and castration resistance. Nature medicine. 2010;16:1414–20.

11. Mulholland DJ, Kobayashi N, Ruscetti M, Zhi A, Tran LM, Huang J, et al. Pten loss and RAS/MAPK activation cooperate to promote EMT and metastasis initiated from prostate cancer stem/progenitor cells. Cancer research. 2012;72:1878–89. [PubMed: 22350410]
12. Ruscetti M, Quach B, Dadashian EL, Mulholland DJ, Wu H. Tracking and Functional Characterization of Epithelial-Mesenchymal Transition and Mesenchymal Tumor Cells during Prostate Cancer Metastasis. Cancer research. 2015;75:2749–59. [PubMed: 25948589]
13. Ruscetti M, Dadashian EL, Guo W, Quach B, Mulholland DJ, Park JW, et al. HDAC inhibition impedes epithelial-mesenchymal plasticity and suppresses metastatic, castration-resistant prostate cancer. Oncogene. 2016;35:3781–95. [PubMed: 26640144]
14. Watson PA, Arora VK, Sawyers CL. Emerging mechanisms of resistance to androgen receptor inhibitors in prostate cancer. Nature reviews Cancer. 2015;15:701–11. [PubMed: 26563462]
15. Carver BS, Chapinski C, Wongvipat J, Hieronymus H, Chen Y, Chandarlapaty S, et al. Reciprocal feedback regulation of PI3K and androgen receptor signaling in PTEN-deficient prostate cancer. Cancer cell. 2011;19:575–86. [PubMed: 21575859]
16. Mulholland DJ, Tran LM, Li Y, Cai H, Morim A, Wang S, et al. Cell autonomous role of PTEN in regulating castration-resistant prostate cancer growth. Cancer cell. 2011;19:792–804. [PubMed: 21620777]
17. Ku SY, Rosario S, Wang Y, Mu P, Seshadri M, Goodrich ZW, et al. Rb1 and Trp53 cooperate to suppress prostate cancer lineage plasticity, metastasis, and antiandrogen resistance. Science. 2017;355:78–83. [PubMed: 28059767]
18. Ammirante M, Luo JL, Grivennikov S, Nedospasov S, Karin M. B-cell-derived lymphotoxin promotes castration-resistant prostate cancer. Nature. 2010;464:302–5. [PubMed: 20220849]
19. Garcia AJ, Ruscetti M, Arenzana TL, Tran LM, Bianci-Frias D, Sybert E, et al. Pten null prostate epithelium promotes localized myeloid-derived suppressor cell expansion and immune suppression during tumor initiation and progression. Molecular and cellular biology. 2014;34:2017–28. [PubMed: 24662052]
20. Huynh H, Ong R, Haike K, Soong R, Petrova E, Liu N. Potent activity of BAY 1082439, a PI3Kα/β balanced inhibitor in gastric cancer models, as single agent and in combination with standard of care. AACR 106th Annual Meeting 2015.
21. Jiao J, Wang S, Qiao R, Vivanco I, Watson PA, Sawyers CL, et al. Murine cell lines derived from Pten null prostate cancer show the critical role of PTEN in hormone refractory prostate cancer development. Cancer research. 2007;67:6083–91. [PubMed: 17616663]
22. Okkenhaug K, Graupera M, Vanhaesebroeck B. Targeting PI3K in Cancer: Impact on Tumor Cells, Their Protective Stroma, Angiogenesis, and Immunotherapy. Cancer discovery. 2016;6:1090–105. [PubMed: 27655435]
23. Massard C, Chi KN, Castellano D, de Bono J, Gravis G, Dirix L, et al. Phase Ib dose-finding study of abiraterone acetate plus buparlisib (BKM120) or dactolisib (BEZ235) in patients with castration-resistant prostate cancer. European journal of cancer. 2017;76:36–44. [PubMed: 28282611]
24. Armstrong AJ, Halabi S, Healy P, Alumkal JJ, Yu EY, Winters C, et al. Phase II trial of the PI3 kinase inhibitor BKM120 with or without enzalutamide in men with metastatic castration resistant prostate cancer (mCRPC). J Clin Oncol. 2015;33.
25. Mateo J, Ganji G, Lemech C, Burris HA, Han SW, Swales KE, et al. A first-time-in-human study of GSK2636771, a phosphoinositide 3 kinase beta-selective inhibitor, in patients with advanced solid tumors. Clinical cancer research : an official journal of the American Association for Cancer Research. 2017.
26. Fruman DA, Chiu H, Hopkins BD, Bagrodia S, Cantley LC, Abraham RT. The PI3K Pathway in Human Disease. Cell. 2017;170:605–35. [PubMed: 28802037]
27. Wang BD, Ceniccola K, Hwang S, Andrawis R, Horvath A, Freedman JA, et al. Alternative splicing promotes tumour aggressiveness and drug resistance in African American prostate cancer. Nature communications. 2017;8:15921.

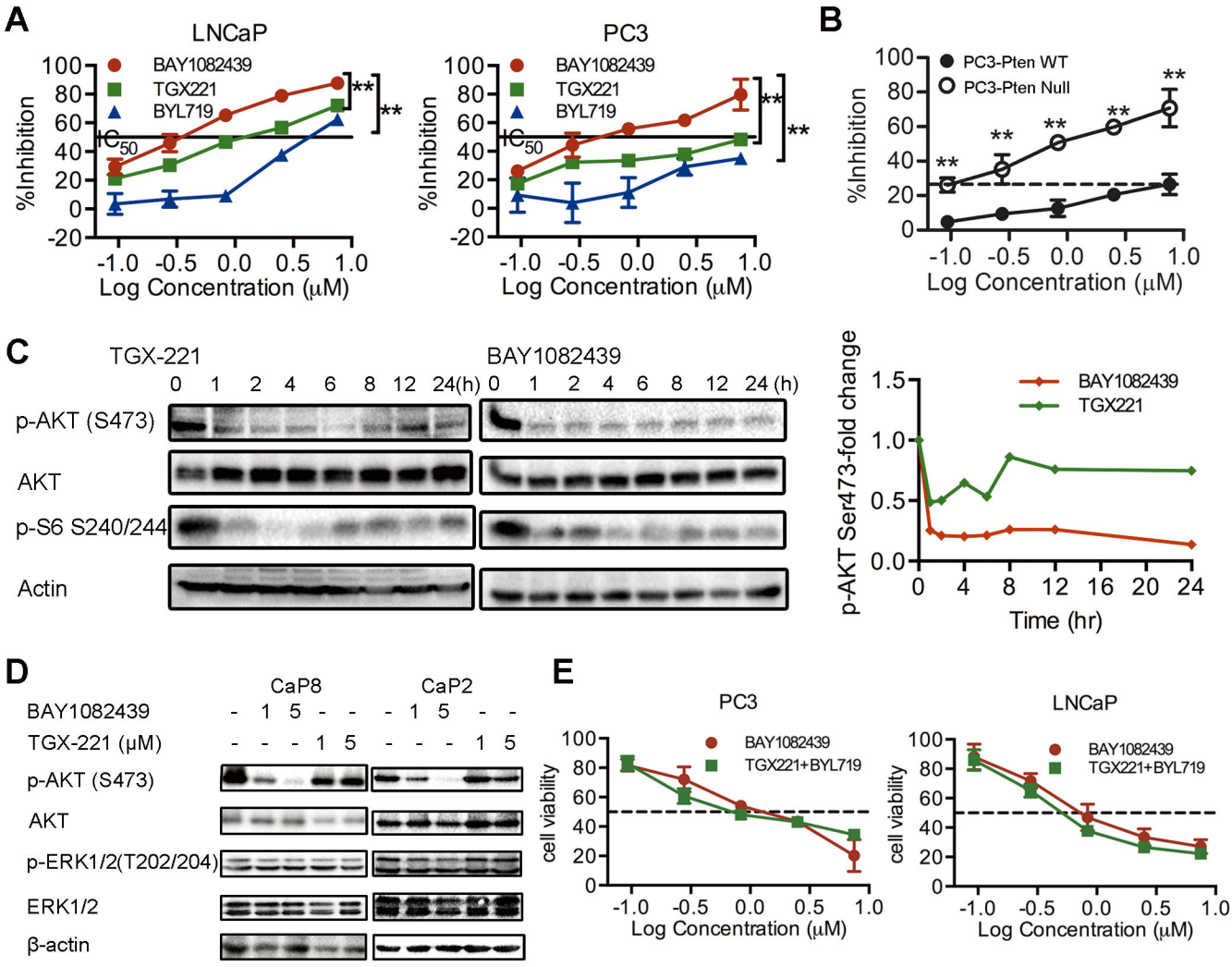

Figure 1. PI3Kα/β dual-balanced inhibitor BAY1082439 inhibits proliferation of *PTEN*-null prostate cells *in vitro*

(A) LNCaP and PC3 cells were treated with BAY1082439, TGX-221 or BYL-719 in different concentrations and the inhibition effects on cell growth were analyzed. (B) PC3-WT and PC3-*PTEN* null cells were treated with BAY1082439 at different concentrations and the effects on cell growth were analyzed. (C) PC3 cells were treated with 1μM TGX-221 or BAY1082439 and the effects on P-AKT (S473) and P-S6 (Ser 240/244) levels were analyzed by Western blot analysis; the fold change in P-AKT (S473) was determined by densitometry analysis using total AKT as loading control. (D) Cap2 and Cap8 cells were treated with BAY1082439 or TGX-221, P-AKT (S473) and P-ERK1/2 (Thr 202/204) levels were analyzed. (E) LNCaP and PC3 cells were treated with BAY1082439 or TGX-221+BYL-719 in different concentrations and cell viability was analyzed. For *in vitro* studies, each data point had 3 replicates and each experiment was repeated at least 3 times. Student's t-test was used for data evaluation. **, $p < 0.01$. BYL-719: PI3Kα inhibitor, TGX-221: PI3Kβ inhibitor.

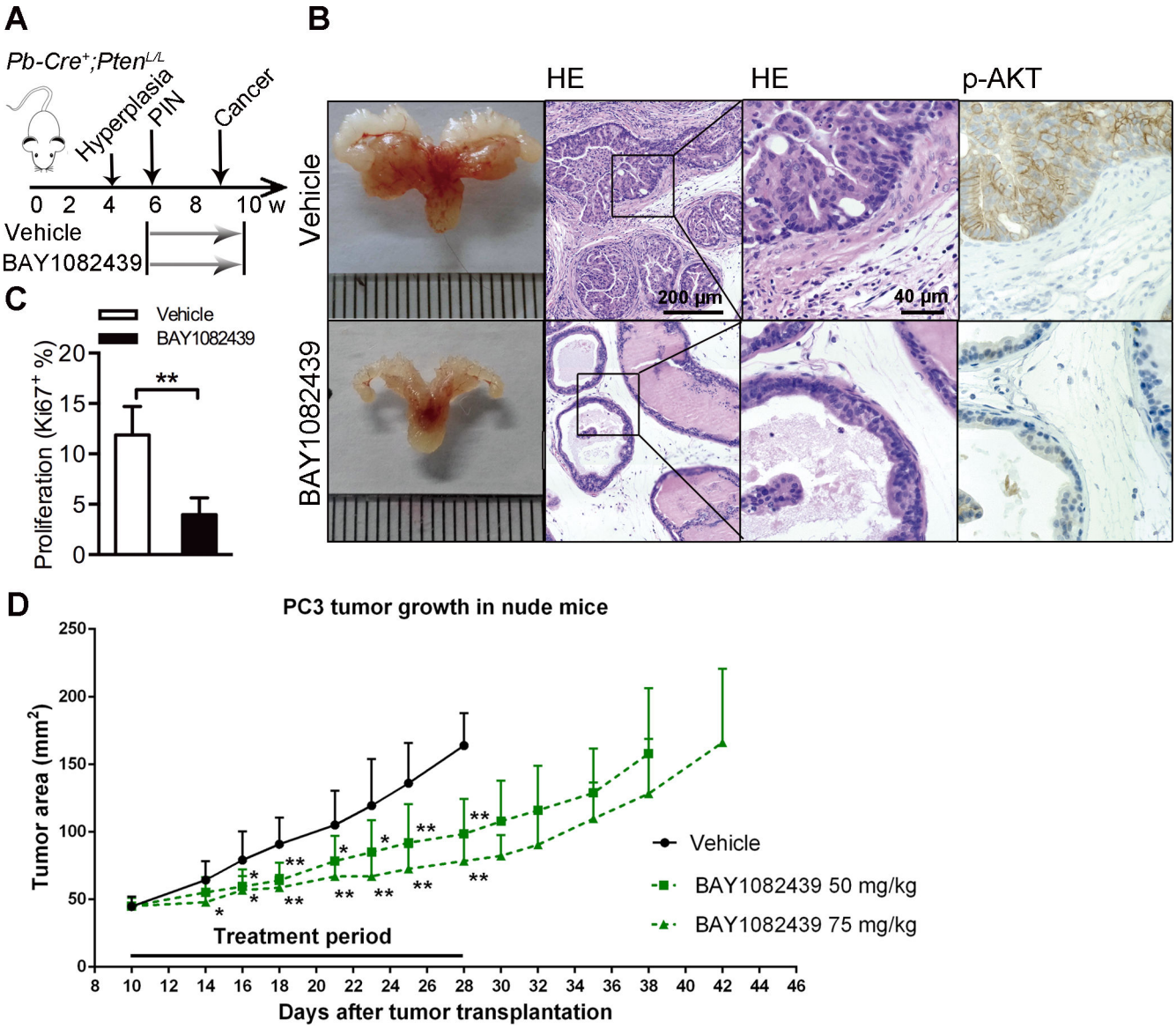

Figure 2. PI3Kα/β dual-balanced inhibitor BAY1082439 inhibits proliferation of *PTEN*-null prostate cells *in vivo*

(A) Experimental setup, (B) HE and immunohistochemistry (IHC) staining, (C) Ki67 index of prostate tumors from mice treated with BAY1082439 (n=6) or vehicle (n=6). (D) The growth curves of PC3 xenograft tumors treated with vehicle (n=8) or BAY1082439 (n=8). Student's t-test was used for data evaluation. **, $p < 0.01$.

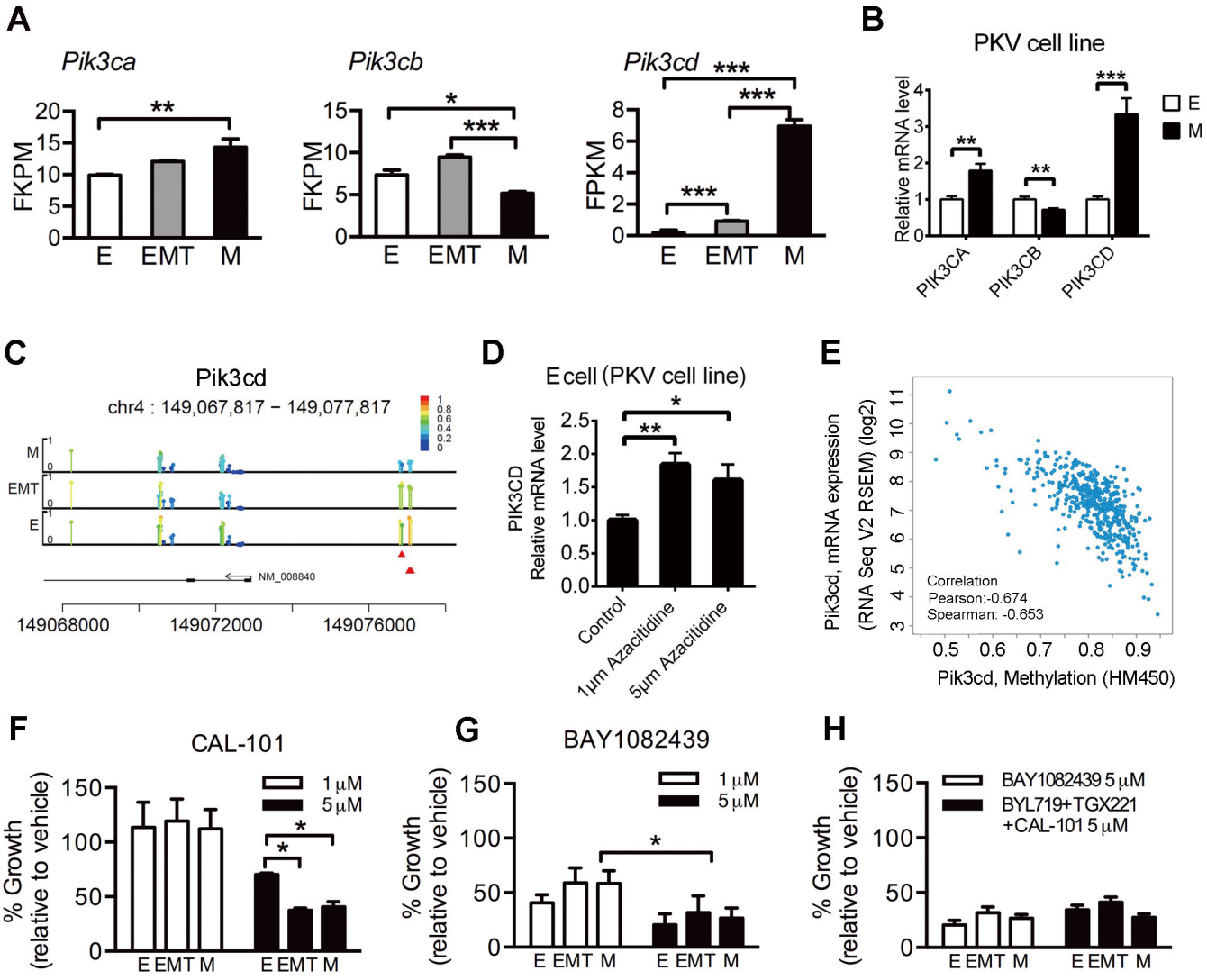

Figure 3. PI3Kδ upregulation is a novel resistance mechanism for EMT and mesenchymal cells and BAY1082439 can target all three tumor cell states

(A) RT-PCR analysis for *Pik3cd*, *Pik3ca* and *Pik3cb* expression levels in FACS-sorted epithelial, EMT and mesenchymal cells from the CPKV tumor cell, (B) and FACS sorted epithelial (E) and mesenchymal (M) cells from PKV cell line. (C) DNA methylation status of *Pik3cd* gene assessed by RRBS in epithelial, EMT and mesenchymal cells. Bar height and color indicate methylation level of each CpG, and each detected CpG was marked with a circle. Red triangle indicates position of DMS; (D) RT-PCR analysis for *Pik3cd* expression levels in E cells from the CPKV tumor cell line after treatment with Azacitidine. (E) Negative correlation between *PIK3CD* gene DNA methylation and mRNA expression in prostate cancer database of TCGA (right panel). PKV cells were treated with (F) CAL-101, (G) BAY1082439 or (H) BYL-719+TGX-221+CAL-101. Cell growth rate in epithelial, EMT and mesenchymal cells was analyzed, Data represent mean ± SD. Student's t-test was used. 3 replicates in each study. *, $p < 0.05$, **, $p < 0.01$. ***, $p < 0.001$.

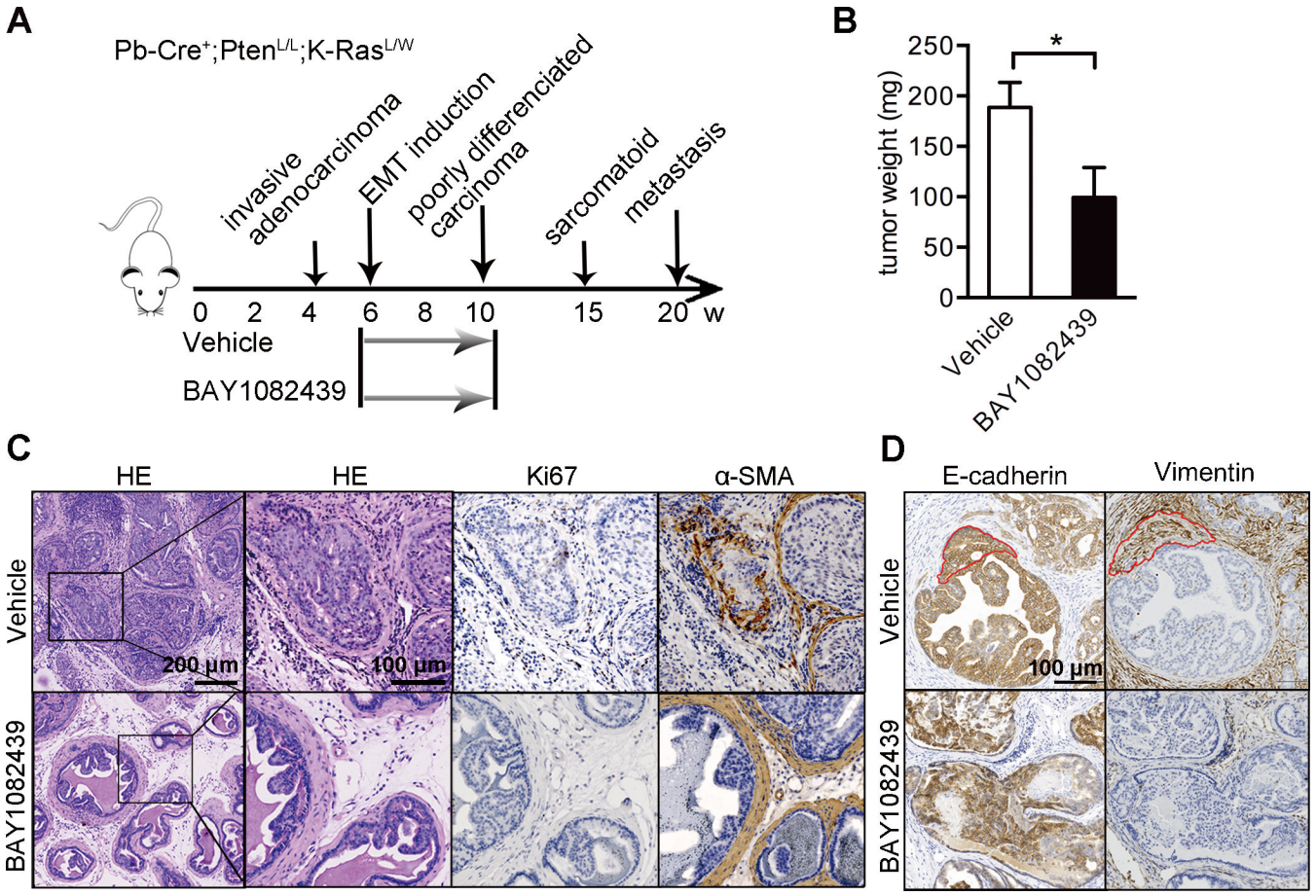

Figure 4. BAY1082439 effectively prevents EMT-mediated invasive carcinoma

(A) Six-week-old CPK mice were treated with vehicle (n=3) or BAY1082439 (n=3). (B) Average prostate weight was analyzed. (C) HE and IHC staining of CPK prostate tumors treated with BAY1082439 or vehicle. (D) IHC staining of E-cadherin and Vimentin from CPK prostate tumors treated with BAY1082439 or vehicle. Data represent mean ± SD. Student's t-test was used. *, $p < 0.05$, **, $p < 0.01$.

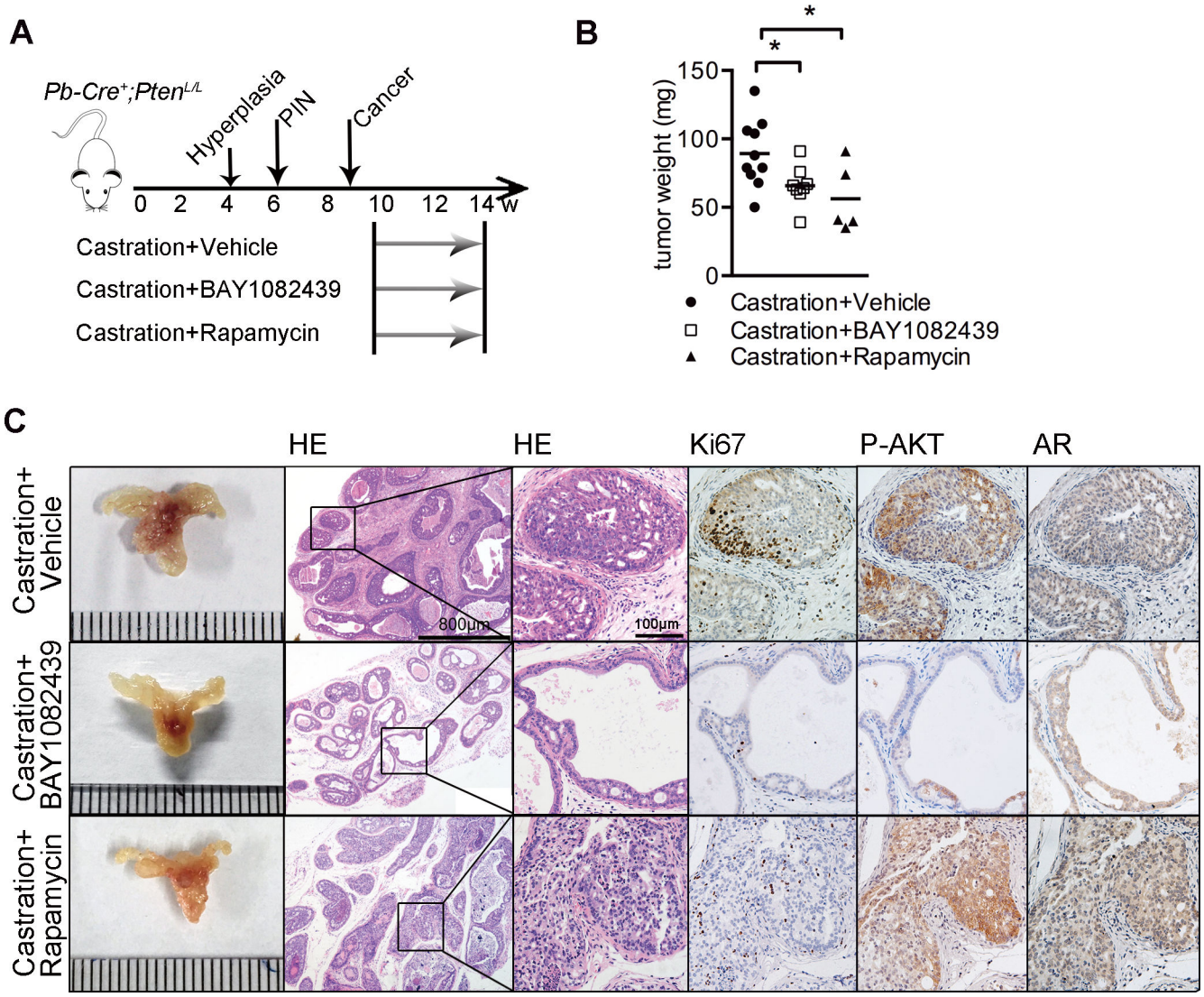

Figure 5. BAY1082439 inhibits CRPC growth

(A) Ten-week-old CP mice were castrated then treated with vehicle (n=10), BAY1082439 (n=8) or rapamycin (n=5); (B) Prostate tumor weight was analyzed; (C) HE and IHC staining of castrated prostate tumors under different treatments. Student's t-test was used. *, $p < 0.05$.

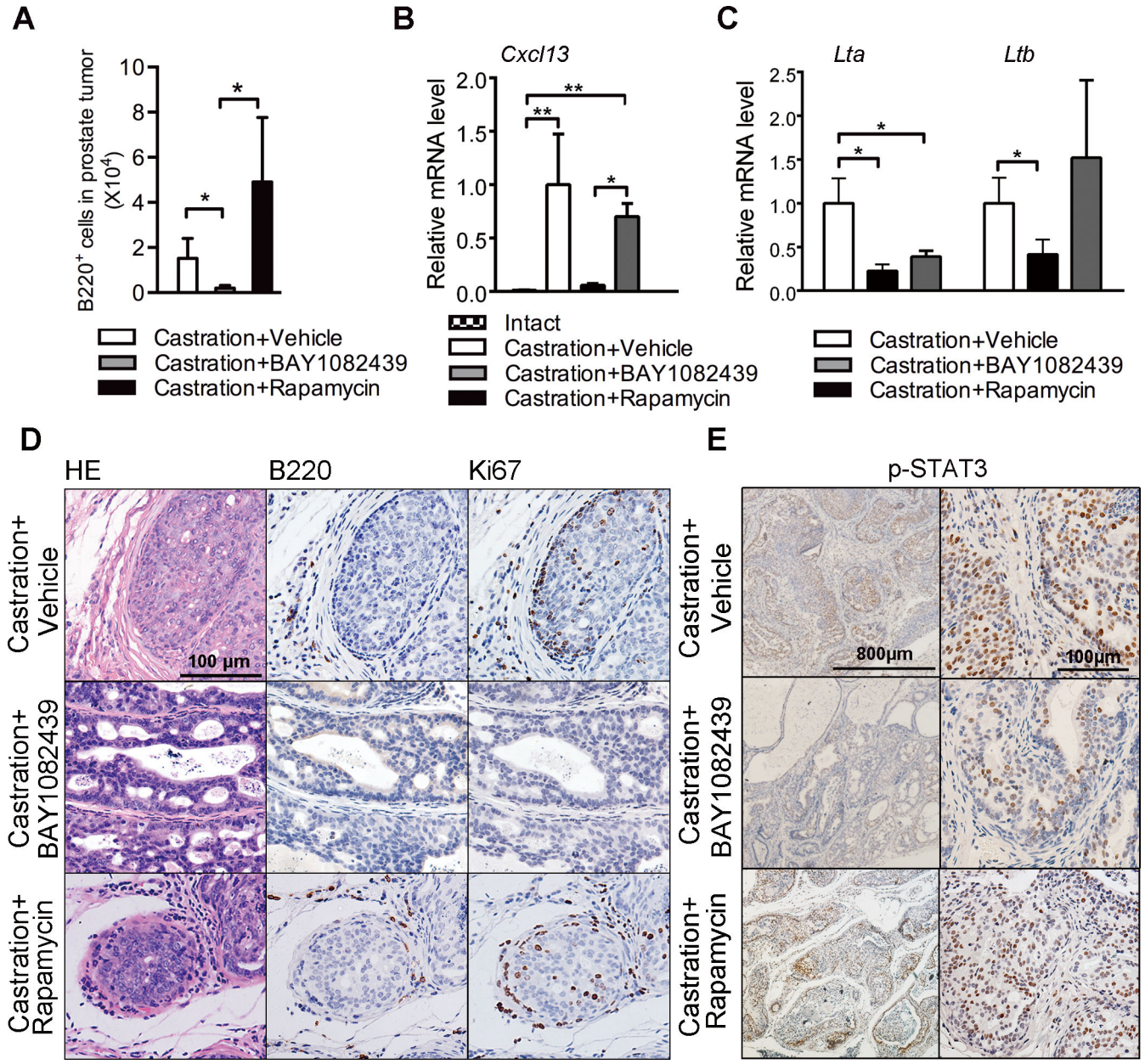

Figure 6. BAY1082439 inhibits CRPC growth by blocking B cell infiltration and lymphotoxin release

(A) Quantitative analysis of prostate tumor infiltrating B cells in animals shown in Fig. 3A; (B) RT-PCR analysis of *CXCL13*, (C) *LTA* and *LTB* expression levels in prostate tumor tissues from intact (n=6) and castrated CP mice treated with vehicle (n=10), BAY1082439 (n=8) and rapamycin (n=5); (D) HE, Ki67, B220 and (E) P-STAT3 IHC staining of prostate tumor tissues from castrated CP mice treated with vehicle, BAY1082439 or rapamycin. Data in A-C are represented as mean ± SD. Two-way ANOVA was used in A. Student's t-test was used in D and E. 3 replicates were analyzed in A-C. *, $p < 0.05$, **, $p < 0.01$